AFRL-OSR-VA-TR-2014-0255

ADAPTIVE PIEZOELECTRIC CIRCUITRY SENSOR NETWORK

KON-WELL WANG
MICHIGAN UNIV ANN ARBOR

09/17/2014
Final Report

Air Force Research Laboratory
AF Office Of Scientific Research (AFOSR)/ RTA
Arlington, Virginia 22203
Air Force Materiel Command

REPORT DOCUMENTATION PAGE

Form Approved
OMB No. 0704-0188

1. REPORT DATE *(DD-MM-YYYY)*	**2. REPORT TYPE**	**3. DATES COVERED** *(From - To)*
09-09-2014	Final Performance Report	06-01-2011 - 05-31-2014

4. TITLE AND SUBTITLE

Adaptive Piezoelectric Circuitry Sensor Network with High-Frequency Harmonics Interrogation for Structural Damage Detection

5a. CONTRACT NUMBER

5b. GRANT NUMBER
FA9550-11-1-0072

5c. PROGRAM ELEMENT NUMBER

6. AUTHOR(S)

Kon-Well Wang and Jiong Tang

5d. PROJECT NUMBER

5e. TASK NUMBER

5f. WORK UNIT NUMBER

7. PERFORMING ORGANIZATION NAME(S) AND ADDRESS(ES)

The Regents of the University of Michigan,
3003 S. State Street,
Room 1056, Ann Arbor, 48109-1274

8. PERFORMING ORGANIZATION REPORT NUMBER

10-PAF05201

9. SPONSORING / MONITORING AGENCY NAME(S) AND ADDRESS(ES)

Dr. David S. Stargel
AF Office of Scientific Research
875 N Randolph St. Room 3112
Arlington, VA 22203

10. SPONSOR/MONITOR'S ACRONYM(S)

AFOSR/RSA

11. SPONSOR/MONITOR'S REPORT NUMBER(S)

12. DISTRIBUTION / AVAILABILITY STATEMENT

Approved for public release

13. SUPPLEMENTARY NOTES

14. ABSTRACT

This research explores structural damage identification via advancing the impedance-based approach. Specifically, we propose to create a new concept of adaptive high-frequency piezoelectric self-sensing interrogation by means of tunable circuitry integration to the piezoelectric transducer. The underlying hypothesis is that, by tuning online the circuitry elements properly, both the quality and the quantity of high-frequency admittance measurement data can be greatly increased for damage detection purpose, which provides a foundation for the subsequent development of new damage identification algorithms. The objective is to fundamentally enhance the identification accuracy and confidence-level by the concurrent advancement of sensing mechanism and inverse identification algorithms. At the sensing mechanism level, new concept of enhanced piezoelectric admittance sensing using circuitry integration is developed, and sensor design guidelines are provided. At the inverse identification methodology level, new algorithms of damage identification are synthesized, which can take full advantage of the new sensing mechanism. These efforts have yielded a complete methodology of adaptive high-frequency piezoelectric self-sensing interrogation.

15. SUBJECT TERMS

16. SECURITY CLASSIFICATION OF:			**17. LIMITATION OF ABSTRACT**	**18. NUMBER OF PAGES**	**19a. NAME OF RESPONSIBLE PERSON**
a. REPORT	**b. ABSTRACT**	**c. THIS PAGE**	SAR		Kon-Well Wang
None	None	None			**19b. TELEPHONE NUMBER** *(include area code)* 734-764-8464

Adaptive Piezoelectric Circuitry Sensor Network with High-Frequency Harmonics Interrogation for Structural Damage Detection

GRANT FA9550-11-1-0072

Final Report (June 1, 2011 to May 31, 2014)

Principal Investigators

Kon-Well Wang
Stephen P. Timoshenko Collegiate Professor of Mechanical Engineering
University of Michigan
Ann Arbor, MI 48109

Jiong Tang
Professor of Mechanical Engineering
University of Connecticut
Storrs, CT 06269

Table of Contents

Objectives

The main challenge in structural health monitoring is to identify the location and severity of small-sized damage at an early stage. The two classical and popular approaches, the vibration-based methods and the ultrasonic wave-based methods, both have limitations. This research explores damage identification via advancing a third type of approach: high-frequency harmonic excitation-based self-sensing, i.e., the impedance-based approach. Specifically, we propose to create a new concept of adaptive high-frequency piezoelectric self-sensing interrogation by means of tunable circuitry integration to the piezoelectric transducer. The underlying hypothesis is that, by tuning online the circuitry elements properly, both the quality and the quantity of high-frequency admittance (i.e., the inverse of impedance) measurement data can be greatly increased for damage detection purpose, which provides a foundation for the subsequent development of new damage identification algorithms. The overarching objective is to fundamentally enhance the identification accuracy and confidence-level by the concurrent advancement of sensing hardware and inverse identification algorithms.

Summary of Efforts

In this project, a series of efforts are undertaken to validate the original hypothesis and to formulate a systematic methodology of high-frequency harmonic response-based damage identification, which includes:

- At the sensing mechanism level, new concept of enhanced piezoelectric admittance sensing using circuitry integration is developed, and sensor design guidelines are provided.
- At the inverse identification methodology level, new algorithms of damage identification are synthesized, which can take full advantage of the new sensing mechanism.

These efforts have thoroughly addressed the research issues outlined in the project proposal, and yielded a complete methodology of adaptive high-frequency piezoelectric self-sensing interrogation.

Descriptions of Accomplishments and New Findings

The timely detection of structural faults in aircraft components has obvious significance to the Air Force. The past decade has witnessed ever-increasing enthusiasm on developing structural health monitoring (SHM) systems that can provide near real-time detection of structural damage. Currently there are two widely studied classes of methods in SHM utilizing structural dynamic responses: the vibration-based and the wave propagation-based methods. In both classes of methods, embedded piezoelectric transducers have been widely used to enable online monitoring of structural health. The piezoelectric transducers possess two-way electro-mechanical coupling (i.e., deforming when subject to electrical excitation, and generating voltage/current when subject to deformation) and behave electrically as capacitors. Owing to these features, when we integrate (bond/embed) a piezoelectric transducer to a structure, the electrical impedance/admittance of the transducer is directly related to the impedance of the underlying structure. This has led to the recent interest in developing another class of embedded SHM methods, the piezoelectric impedance/admittance-based methods.

The piezoelectric impedance- or admittance-based approach appears to be quite promising because of the following reasons: 1) Compared to the vibration-based methods, the piezoelectric impedance/admittance can be extracted in high-frequency range (e.g., higher than 30 kHz), which is important for detecting small-sized damage; and 2) Compared to the wave-propagation methods, the impedance/admittance is extracted from the stationary responses (i.e., harmonic responses), and thus is better suited for damage identification (i.e., identifying both the damage location and severity). On the other hand, it is worth noting that while the piezoelectric impedance or admittance-based approach holds great potential, the reality is that such potential has not been fully realized. There appear to be severe bottlenecks: 1) While actual detection sensitivity hinges upon the scale of difference in the measurements upon the occurrence of damage, the response anomaly can still be buried in the measurement noise because different damage profiles affect the responses differently; 2) These methods generally have limitation of inaccuracy due to under-determined inverse problem for damage prediction, especially under noise influences; and 3) Current practices mainly resort to ad hoc damage metrics, i.e., to declare damage occurrence if the difference between the online impedance/admittance measurement and the healthy baseline exceeds a certain threshold, and are still unable to accurately identify damage location and severity.

Based upon the state-of-the-art review and the PIs' experience, we have recognized that some characteristics of the piezoelectric circuitry can be utilized to revolutionize the piezoelectric impedance/admittance sensing. In particular, we propose to integrate tunable circuitry with the piezoelectric transducer to realize dynamical tailoring of the sensing system to fundamentally enhance the sensitivity and robustness. The major accomplishments and new findings garnered throughout this project are summarized in the following sections.

Part I. Integration of adaptive circuitry to enhance the quality and quantity of impedance measurements

In this first part of research, we explore the fundamental sensing mechanism enhancement by circuitry integration. For simplicity in discussion, here we use a one degree-of-freedom (DOF) model to represent the interested mode of the mechanical structure. The dynamic equations of the structure coupled with the piezoelectric transducer without and with the inductance can be derived as

$$m\ddot{q} + c\dot{q} + kq + k_1 Q = 0, \qquad R\dot{Q} + k_2 Q + k_1 q = V_i \qquad \text{(without inductance)} \quad \text{(1a,b)}$$

$$m\ddot{q} + c\dot{q} + kq + k_1 Q = 0, \qquad L\ddot{Q} + R\dot{Q} + k_2 Q + k_1 q = V_i \qquad \text{(with inductance)} \quad \text{(2a,b)}$$

where q is the mechanical displacement, Q is the electrical charge in the circuit, m, c, and k are the mass, damping, and stiffness, respectively; $k_2 = 1/C_p$ is the inverse of the piezoelectric capacitance, and V_i is the excitation voltage. Both systems include a resistor that enables the direct measurement of current resulted from the voltage excitation. The piezoelectric admittances can be expressed as, respectively,

$$\hat{Y}_p = \frac{\hat{I}}{\hat{V}_i} = \frac{i\omega\left(-m\omega^2 + ic\omega + k\right)}{\left(iR\omega + k_2\right)\left(-m\omega^2 + ic\omega + k\right) - k_1^{\,2}} \qquad \text{(without inductance)} \qquad (3)$$

$$\hat{Y}_p = \frac{\hat{I}}{\hat{V}_i} = \frac{i\omega\left(-m\omega^2 + ic\omega + k\right)}{\left(-L\omega^2 + iR\omega + k_2\right)\left(-m\omega^2 + ic\omega + k\right) - k_1^{\,2}} \qquad \text{(with inductance)} \qquad (4)$$

While the impedance and the admittance are inverse with each other, in this research we focus on the admittance, because, as shown in the comparison between Eqs. (3) and (4), the admittance measurements can be greatly impacted by the circuitry dynamics. Indeed, one can see that Eq. (4) is a fourth-order system with two resonances, while Eq. (3) is essentially a second-order system with one resonance since, compared to k_2, $R\omega$ is very small. Obviously, one major difference between the new sensor with the inductance (Eq. (4)) and the traditional approach (Eq. (3)) is that the inductive circuitry introduces an additional DOF, which leads to a new resonant effect in the admittance curve. It is well known that the damage-induced changes are most significant around the resonant peaks. Our preliminary investigation indicated:

- The circuitry resonance effect, if properly utilized, may amplify, under the same level of voltage excitation, the magnitude of the admittance. Furthermore, it may even amplify the damage-induced admittance *change*.
- Through tuning the inductance to different values, we can obtain a much enlarged dataset for damage detection, which consists of *a family of* admittance curves (under different inductance values) as compared to the original single admittance curve obtained by the fixed sensor without circuit.

The new idea introduced in this part of research is to integrate a negative capacitance into the circuit. In this case, we can obtain the electrical admittance of the enhanced series circuitry, normalized by the electrical admittance of the stand-alone piezoelectric transducer (before it is integrated onto the mechanical structure), which is $\hat{Y}_P = i\omega / k_2$, as

$$\frac{\hat{Y}_N}{\hat{Y}_P} = \frac{k_2\left(-m\omega^2 + ic\omega + k\right)}{\left(-L\omega^2 + iR\omega + \hat{k}_2\right)\left(-m\omega^2 + ic\omega + k\right) - k_1^{\,2}} \qquad (5)$$

The above expression can be can be written as

$$\frac{\hat{Y}_L}{\hat{Y}_P} = \frac{\delta^2\left(1 + 2\varsigma i\Omega - \Omega^2\right)}{\left(1 + 2\varsigma i\Omega - \Omega^2\right)\left(\delta^2 + r\delta^2 i\Omega - \Omega^2\right) - \delta^2\xi^2} \qquad (6)$$

where

$$\omega_m = \sqrt{\frac{k}{m}},\ \omega_e = \sqrt{\frac{k_2}{L}},\ \Omega = \frac{\omega}{\omega_m},\ \delta = \frac{\omega_e}{\omega_m},\ \varsigma = \frac{c}{2m\omega_m},\ r = \frac{R}{k_2}\omega_m,\ \hat{\xi} = \frac{k_1}{\sqrt{k\hat{k}_2}} \qquad (7a\text{-}g)$$

Here ω_m, ω_e, Ω, δ, ς, r and ξ are the mechanical modal frequency, the electrical circuitry resonant frequency, the non-dimensionalized excitation frequency, the ratio between the electrical resonant frequency and the mechanical modal frequency (i.e., inductance tuning ratio), the structural damping ratio, the electrical damping/resistance ratio, and the generalized electro-mechanical coupling coefficient, respectively. Without loss of generality, the structural damping ratio is set as $\varsigma = 0.001$. Clearly, after the negative capacitive element is integrated, the inverse of the overall capacitance in the circuit is reduced, and hence the generalized electro-mechanical coupling coefficient is increased, i.e., $\hat{\xi} > \xi$.

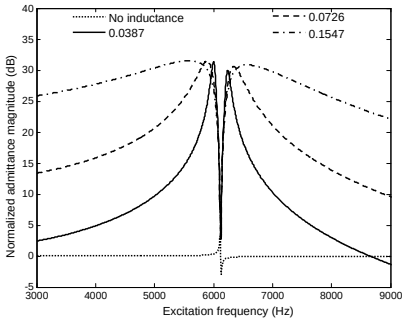

Figure 1 Circuitry admittance curves under different generalized coupling coefficients.

The circuitry admittance curves of the benchmark undamaged beam with different generalized coupling coefficients are shown in Figure 1. The coupling coefficients are 0.0387, 0.0726 and 0.1547, which correspond to the cases without the negative capacitance (piezoelectric inductive circuitry), with a -12.39 nF negative capacitance, and with a -9.46 nF negative capacitance, respectively. Consider the 17th mechanical modal frequency (6120 Hz). In order to have $\delta = 1$ (to achieve large dynamic coupling between the transducer and the host structure), under these coupling coefficients, the inductance values are selected as 76.2 mH, 21.65 mH and 4.75 mH (which are actually the frequency-veering inductance values under these three coupling coefficients, correspondingly. For reference, the admittance curve extracted by the low-cost impedance measurement circuit (without the tunable inductance and negative capacitance) is also plotted. It can be seen that the larger the coupling coefficient, the flat the admittance curve is whereas the resonant peaks remain about the same. For example, when the system is excited at 4 kHz, if we integrate a negative capacitive element with a 0.0726 coupling coefficient, the admittance magnitude is 15.83 dB, which is 10.96 dB larger than that without the negative capacitance (4.87 dB). When we connect a negative capacitive element corresponding to a larger coupling coefficient ($\hat{\xi} = 0.1547$), the increased admittance magnitude is 22.85 dB, compared with the result without the negative capacitance. This means that the admittance magnitude remains at a high level in a much wider frequency range around the resonant peaks of the admittance curve, when larger coupling coefficient is selected. Therefore, the negative capacitive element can further increase the signal-to-noise ratio in sensor measurement, compared with the preliminary study.

The more important effect of the negative capacitive element can be seen in the change of admittance signature when damage occurs. This is because the larger the change of admittance under damage occurrence, the more sensitive the damage detection scheme is. In this research, the structural damage is assumed to cause the loss of beam equivalent modal stiffness (k), and the severity of damage is defined as its percentage change. After a 1% beam modal stiffness loss occurs, the changes of the admittance under different coupling

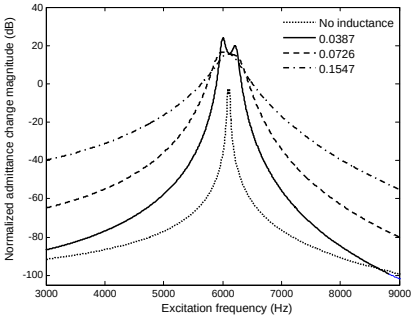

Figure 2 Circuitry admittance change curves under different generalized coupling coefficients.

coefficients are shown in Figure 2. We can see that the larger the coupling coefficient, the flat the curve of admittance change is whereas the peaks are reduced only slightly. For example, with the voltage excitation frequency at 5 kHz, the magnitude of admittance change is increased 21.93 dB after a -12.39 nF negative capacitance is connected ($\bar{\xi} = 0.0726$). If the negative capacitance with a larger coupling coefficient (-9.46 nF and $\bar{\xi} = 0.1547$) is integrated, the increased admittance change at this frequency is 42.77 dB. It is well known that in the impedance/admittance based sensory system, there exist frequency shifts and magnitude changes in the piezoelectric impedance or admittance curves after the structural damage occurrence, and these changes are most significant around the resonant peaks. Therefore, the negative capacitive element can enrich the input information for the damage detection and identification, and hence improve the detection accuracy and sensitivity.

Part II. Analysis on the adaptive piezoelectric circuitry for data enrichment

This part of the research develops the damage identification algorithm which exploits the enriched admittance information obtained by employing the adaptive piezoelectric circuitry. Numerical analysis is performed by using the spectral element method (SEM), and experimental investigation clearly verified the effectiveness of the proposed methodology. Figure 3 shows the schematic of an example structure integrated with adaptive piezoelectric circuit for data enrichment. The piezoelectric transducer on the P_1 th element of the beam structure is used for piezoelectric impedance measurement, and another transducer with tunable inductor is implemented on the P_2th element for data enrichment.

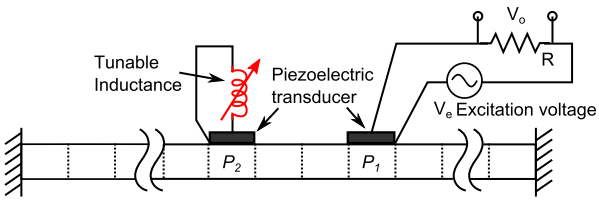

Figure 3 Illustration of the structure integrated with the adaptive piezoelectric circuitry.

First, the transducer on the P_1th element is only considered in the analysis. As we assume that the structural damage is represented by the element bending stiffness reduction, the piezoelectric admittance of the healthy and damaged structures can be formulated as $Y(\omega)$, $\hat{Y}(\omega)$ by using spectral element model, respectively.

$$Y(\omega) = \frac{1}{R} K_2 \left[K_1 \mathbf{\Phi}_p \mathbf{S}^{-1}(\omega) \mathbf{\Phi}_p^T + 1 \right] \tag{8}$$

$$\hat{Y}(\omega) = \frac{1}{R} K_2 \left[K_1 \mathbf{\Phi}_p [\mathbf{S}^{-1}(\omega) + \mathbf{S}^{-1}(\omega) [\textstyle\sum_{i=1}^{N} \mathbf{C}_i^T \mathbf{K}_{ei} \mathbf{C}_i d_i] \mathbf{S}^{-1}(\omega)] \mathbf{\Phi}_p^T + 1 \right] \tag{9}$$

$$K_1 = \frac{h_b b_p (E_p d_{31})^2}{4 \varepsilon_{33}^T l_p (1 + i\omega R C_p)} \left[\left(\frac{1}{2}(h_p + h_b) \right)^2 - \left(\frac{1}{2} h_b \right)^2 \right], \; K_2 = \frac{i\omega R C_p}{1 + i\omega R C_p} \tag{10a,b}$$

where ε_{33}^T, l_p, b_p, h_p, d_{31}, E_p, and C_p are the permittivity, length, width, thickness, piezoelectric coefficient, elastic modulus, and capacitance of the piezoelectric transducer, respectively. h_b is the thickness of the beam, ω is the excitation frequency, and R is the resistance. $\mathbf{S}(\omega)$ is the dynamic stiffness matrix of the beam structure formulated by the SEM. $\mathbf{\Phi}_p$ indicates the location of the transducer at the P_1th element, and d_i is the stiffness reduction of the ith element. $\mathbf{C}_i$ is the connectivity matrix for assembling elemental matrices, and $\mathbf{K}_{ei}$ is the ith elemental stiffness matrix formulated by finite element method, which is used to approximate the partial derivative

of the damaged stiffness matrix inverse $\hat{\mathbf{S}}^{-1}(\omega)$. The first-order sensitivity equation that directly relates the difference of the undamaged and damaged piezoelectric admittance $\Delta\boldsymbol{Y}$ with damage indices can be derived as the following.

$$\Delta\boldsymbol{Y} = \frac{1}{R}K_1K_2\boldsymbol{\Phi}_p[\mathbf{S}^{-1}(\omega)[\sum_{i=1}^{N}\mathbf{C}_i^T\mathbf{K}_{ei}\mathbf{C}_i d_i]\mathbf{S}^{-1}(\omega)]\boldsymbol{\Phi}_p^T = \mathbf{G}\times\mathbf{d} \tag{11}$$

$$\Delta\boldsymbol{Y} = \left[\hat{Y}(\omega_1), \hat{Y}(\omega_2), \dots, \hat{Y}(\omega_m)\right]^T - [Y(\omega_1), Y(\omega_2), \dots, Y(\omega_m)]^T \tag{12a}$$

$$G_{ji} = \frac{1}{R}K_1K_2\boldsymbol{\Phi}_p\left[\boldsymbol{S}^{-1}(\omega_j)\mathbf{C}_i^T\boldsymbol{K}_{ei}\mathbf{C}_i\mathbf{S}^{-1}(\omega_j)\right]\boldsymbol{\Phi}_p^T \quad i=1, 2, \dots, N \text{ and } j=1, 2, \dots, m \tag{12b}$$

$$\mathbf{d} = [d_1, d_2, \dots, d_N]^T \tag{12c}$$

where m is the number of admittance measurements and N is the number of elements in the model. The location and severity of damage can be identified by solving the damage index vector **d**. However, in most practical cases, **d** cannot be uniquely obtained and becomes highly sensitive to measurement errors since the sensitivity matrix **G** is rank deficient, i.e. $m < N$.

This concern of under-determined inverse problem is addressed by implementing the concept of adaptive piezoelectric circuitry for impedance data enrichment. As we implement additional piezoelectric transducer with tunable inductor L as shown in Figure 3, a new degree of freedom is created by the circuit elements into the integrated system. By selectively tuning the inductance values, the dynamics of the coupled system can be continuously and systematically modified, which enables to obtain different impedance responses with respect to same structural damage. The modified stiffness matrix $\mathbf{S}_{new}$ of the integrated system can be obtained as following.

$$\mathbf{S}_{new} = \mathbf{S} - K_{1A}\boldsymbol{\Phi}_{p_2}^T\boldsymbol{\Phi}_{p_2} \tag{13}$$

$$K_{1A} = \frac{h_b b_p (E_p d_{31})^2(\omega^2 L C_{p_2})}{4\varepsilon_{33}^T l_p(1-\omega^2 L C_{p_2})}\left[\left(\frac{1}{2}(h_p + h_b)\right)^2 - \left(\frac{1}{2}h_b\right)^2\right] \tag{14}$$

where $\boldsymbol{\Phi}_{p_2}$ and C_{p_2} indicate the location and capacitance of the additional piezoelectric transducer, respectively. The inverse equation for the integrated system can be similarly formulated.

$$\Delta\boldsymbol{Y}_{new} = \frac{1}{R}K_1K_2\boldsymbol{\Phi}_p[\mathbf{S}_{new}^{-1}(\omega)[\sum_{i=1}^{N}\mathbf{C}_i^T\mathbf{K}_{ei}\mathbf{C}_i d_i]\mathbf{S}_{new}^{-1}(\omega)]\boldsymbol{\Phi}_p^T = \mathbf{G}_{new}\times\mathbf{d} \tag{15}$$

$$\Delta\boldsymbol{Y}_{new}(\omega) = \widehat{\boldsymbol{Y}}_{new}(\omega) - \boldsymbol{Y}_{new}(\omega) \tag{16a}$$

$$G_{new\,ji} = \frac{1}{R}K_1K_2\boldsymbol{\Phi}_p\left[\mathbf{S}_{new}^{-1}(\omega_j)\mathbf{C}_i^T\mathbf{K}_{ei}\mathbf{C}_i\mathbf{S}_{new}^{-1}(\omega_j)\right]\boldsymbol{\Phi}_p^T \quad \text{i=1, 2, …, N and j=1, 2, …, m} \tag{16b}$$

When the inductance is tuned to form a sequence from L_1 to L_P, we can derive a family of P different inverse equations and augment them in the matrix form as following.

$$\Delta\boldsymbol{Y}_{sum} = \mathbf{G}_{sum}\times\mathbf{d} \tag{17}$$

$$\Delta \boldsymbol{Y}_{sum} = \begin{Bmatrix} \Delta \boldsymbol{Y}_{new}(L_1) \\ \Delta \boldsymbol{Y}_{new}(L_2) \\ \vdots \\ \Delta \boldsymbol{Y}_{new}(L_P) \end{Bmatrix}, \mathbf{G}_{sum} = \begin{bmatrix} \mathbf{G}_{new}(L_1) \\ \mathbf{G}_{new}(L_2) \\ \vdots \\ \mathbf{G}_{new}(L_P) \end{bmatrix} \quad (18a,b)$$

Equation (17) shows the merit of using adaptive piezoelectric circuitry. The original sensitivity matrix $\mathbf{G}_{new}$ (m by N) is rank deficient, i.e. $m < N$. As P different inductance values are applied to the circuitry, the number of impedance measurements and the sensitivity matrix is greatly enriched up to $P \times m$, thus the originally ill-posed inverse problem is significantly improved.

Numerical analysis on the damage identification using adaptive piezoelectric circuitry

In this section, damage identification studies are provided to examine the viability of the proposed approach for impedance data enrichment. The configuration of the illustrative system is given in Figure 3. A fixed-fixed beam is divided into 31 elements, and piezoelectric transducers are integrated at the 3rd and 21st element. The dynamics of the integrated system is altered by the adaptive piezoelectric circuitry at the 3rd element, and the other transducer is utilized for impedance measurement. Some relevant system parameters are presented in Table 1. In this analysis, Tikhonov regularization is employed to solve the inverse problems.

In the first case study, the damage is assumed as 10% stiffness reduction on the 13th element. Random noise of 62 dB signal-to-noise ratio (SNR) is added to the impedance response. Since the damage effect is more significant near resonance peaks, the impedance changes around each resonance peak are utilized for the damage identification. Then, the inductances are tuned once for each resonance peak to enrich the impedance measurements. Table 2 provides 8 inductances selected for all resonant frequencies in the frequency range of 5 kHz to 11 kHz.

Table 1 System parameters

Beam structure		Piezoelectric material	
Length × Thickness × Width, mm	607.8 × 7.62 × 3.175	Length × Thickness × Width, mm	17 × 7.62 × 0.191
Young's modulus, GPa	73.4	Young's modulus, GPa	66
Density, kg/m^3	2780	Density, kg/m^3	7800
Loss factor, %	0.15	Permittivity, ε_{33}^{T} , F/m	1.6×10^{-8}
Poisson's ratio	0.33	Piezoelectric constant, d_{31}, m/V	-190×10^{-12}

Table 2 Inductance values selected for each resonance peak

Resonant frequency, kHz	5.39	6.05	6.75	7.49	8.26	9.06	9.91	10.79
Inductance, mH	134.6	106.4	85.1	68.9	56.4	46.6	38.8	32.6

As we utilize these enriched impedance measurements, the total number of piezoelectric impedance data set can be increased by 8 times in this case study. A comparison of the damage prediction results with and without this impedance data enrichment is provided in Figure 4. The horizontal axis is the element number and the damage index, stiffness reduction of the element, is provided along the vertical axis. The dotted line shows the actual damage distribution. It can be observed that the result obtained by traditional method without data enrichment cannot accurately identify damage characteristics due to its severely ill-posed inverse equation, even with a low level of additive noise (62 dB SNR). However, when the proposed method of

adaptive circuitry is applied, the damage identification result indicates approximately 10% stiffness reduction at the 13th element. The root mean square deviation (RMSD) between the predicted stiffness loss **d** and the actual damage $\mathbf{d}^0$ is employed to quantify the prediction error and compare the performance of damage identification.

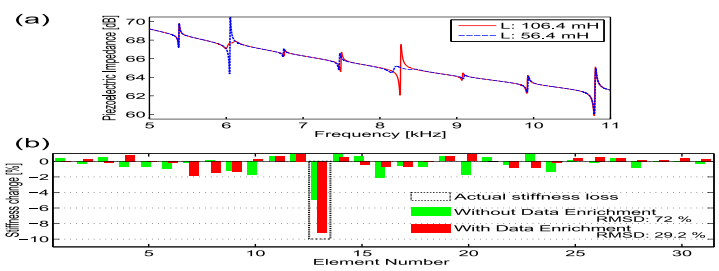

Figure 4 Identification of damage on the 13th element of the example beam structure with 10% stiffness reduction.

$$RMSD = \sqrt{\sum_{i=1}^{N}\left(d_i - d_i^0\right)^2 \Big/ \sum_{i=1}^{N} d_i^{0\,2}} \tag{19}$$

where d_i, d_i^0 are the predicted and actual damage indices of the *i*th element, respectively. When the adaptive circuitry is applied, the RMSD is reduced from 72 % to 29.2 %.

Another numerical case study is conducted with multiple damages. The structural damages are assumed to be 5 % and 8 % stiffness reductions at the 13th and 18th elements, respectively. In this case, higher level of noise (36 dB SNR) is added in the impedance response. Figure 5 shows the damage prediction result. Without the adaptive circuitry, the damaged elements are virtually indistinguishable, and the result falsely predicts the largest two damages on the 15th and 18th elements with approximately 2 % stiffness reduction. However, as inductance tunings are applied, both damage indices at the 13th and 18th elements clearly indicate the simulated damages in the structure. The damage identified by using the traditional method has 85.6 % of the RMSD error, whereas the proposed approach shows the RMSD of 54.7 %.

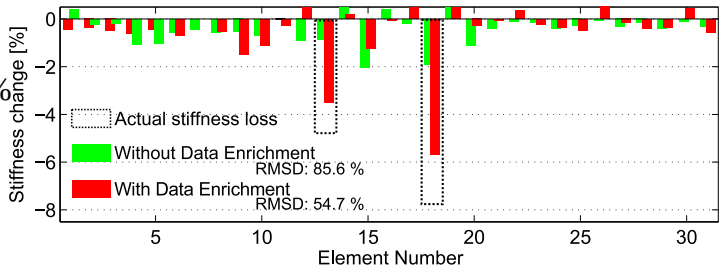

Figure 5 Multiple damage identification on the 13th, 18th elements of the beam with 5%, 8% stiffness reduction, respectively.

Investigation on the number of inductance tunings

Singular value decomposition is conducted to examine how the number of inductance tunings affects the condition of the augmented sensitivity matrix. A case study is performed at the frequency range of 5 kHz to 11 kHz, which contains 8 resonance frequencies, and here we increased the number of inductance tunings to 20. The inductance values are first selected to match the electrical resonance of the adaptive piezoelectric circuitry with each structural resonance of the host structure in the interested frequency range as shown in Table 1. The next tuning values are deviated ± 1 % from the previously selected inductances for resonances, and then ± 2 %, and so on.

Figure 6(a) presents the logarithm of the singular values of the augmented sensitivity matrix $\mathbf{G}_{sum}$ in equation (17). As shown in the figure, the singular values are greatly increased overall when the first 8 inductances are applied for impedance data enrichment, and they increased even

more as the number of inductance tunings is increased to 20. This implies that the ill-posed sensitivity matrix can be improved as more inductance tunings are applied. As a result, the damage prediction error (RMSD) decreases when more inductance tunings are introduced in the system as shown in Figure 6(b). We can notice that the damage identification error dramatically decreases for the first several inductance tunings, and then decreases gradually afterwards.

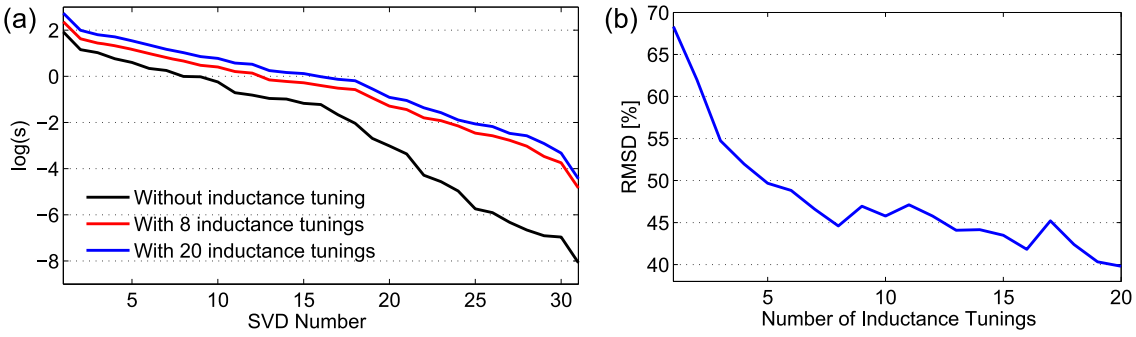

Figure 6 (a) Singular values of the augmented sensitivity matrix when different numbers of inductance tunings are employed. (b) Damage prediction error (RMSD) with respect to the number of inductance tunings.

Same analysis is conducted on other cases with 4 resonances in the frequency range from 8 kHz to 11 kHz, and 12 resonances in the range of 4 kHz to 13 kHz to investigate whether the damage prediction errors decrease similarly in other frequency ranges. All three case studies are repeated 5 times, and the average damage prediction errors for each case are compared in Figure 7. The highlighted boxes in the figure show that the RMSD starts to decrease gradually from near the 4^{th}, 8^{th}, and 12^{th} inductance tuning augmentations when there are 4, 8, and 12 resonances in the interested frequency ranges, respectively. These results indicate that there appears to be a relation between the number of inductance tunings and resonances employed for damage identification. This can be explained by examining how the inductance values are selected, and how they affect the inverse equation from the case study of 8 resonances as an example. As described previously, the first 8 inductance values are tuned to each structural resonance, and then the next inductance values are varied from these values. When the inductances are tuned for each resonant frequency, the piezoelectric impedances of the integrated system are altered distinctively from each other. As these responses are arranged in the form of equation (17), we can fully exploit the merit of data enrichment by augmenting unique and independent information into the sensitivity matrix. Therefore, we can greatly improve the ill-posedness of the inverse equation, which results in notable decrease of the damage prediction error. However, the next groups of inductances are variations from the first group of 8 inductances, thus the corresponding impedance responses are variations of the first group of impedance responses. This set of inductances adds

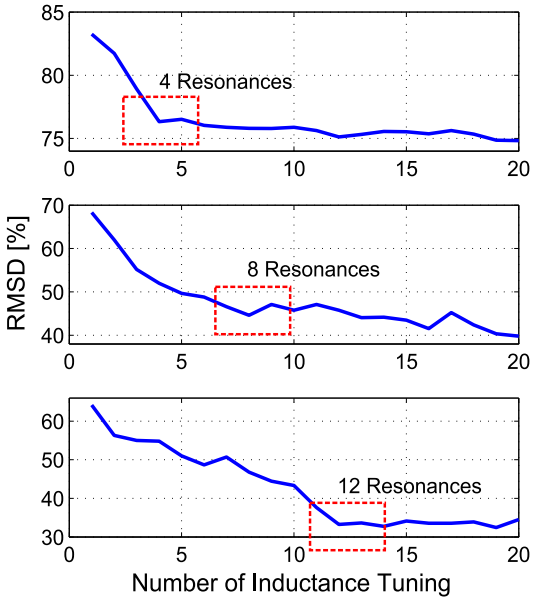

Figure 7 Damage prediction error (RMSD) comparisons for frequency ranges with different number of resonances.

analogous information to the sensitivity matrix, and thus the ill-posedness is improved gradually. For this reason, the damage identification error decreases gradually near after the 8th inductance tunings. From these results, we can conclude that applying more inductance tunings can increase the accuracy in damage prediction by improving the ill-posed nature of the sensitivity matrix. On the other hand, it is suggested that the inductance can be tuned once for each resonance in the frequency range of interest to efficiently exploit the benefit of data enrichment in damage identification.

Experimental Validation

A fixed-fixed aluminum beam (Al-2024) discretized into 61 elements is used in this analysis, and two piezoelectric transducers (PSI-5A4E) are bonded on the top surface of the 29th and 41st elements for inductance tuning and impedance measurement purposes, respectively. We introduced damage as a surface notch at the 25th element of the beam structure for the damaged case. The notch is 0.09 mm deep (2.8% of the beam thickness) and 10.4 mm long having same width of the beam, which results in 8.3% reduction of the local bending stiffness. The experimental configuration including the location of the piezoelectric transducers and damage is presented in Figure 8. A tunable inductor used in this study is realized by op-amps (LM324), resistors, and capacitors. Table 3 provides the relevant parameters and the seven inductance tunings employed for data enrichment. The baseline model is tailored by modifying the length, mechanical loss factor of the beam, and the location of the piezoelectric transducers to minimize the measurement errors of the beam dimensions and material properties in modeling. The measurement noise is 42 dB SNR, however considering the uncertainty in the baseline model, the total noise level can increase. In this analysis, the damage indices are solved by using least-square algorithms with negative constraints. The coefficients are restricted to be negative since we assumed damage as stiffness reduction by designing surface notch in the experiment.

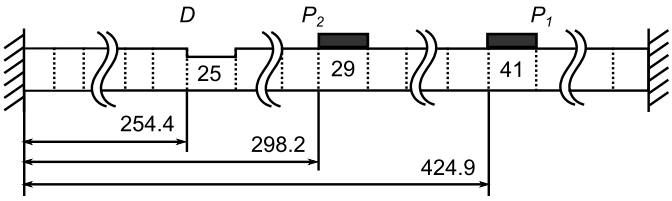

Figure 8 Configuration of the experimental beam structure (measured in millimeters).

Table 3 Parameters of the tunable inductor, beam structure, and piezoelectric transducers

Beam, mm	627.2 × 7.21 × 3.175		P_1, mm	16.85 × 7.09 × 0.191		P_2, mm	16.3 × 7.09 × 0.191	
Circuitry element	C_1 ,nF	C_2, nF	R_2, Ω	R_3, Ω	R_4, Ω	R_5, Ω	R_6, Ω	R_7, Ω
	9.788	9.807	4620	4629	4629	4628	4632	4629
	L, mH	39.45	40.367	41.272	45.32	46.16	63.1	80.12
	R_1, Ω	850	870	890	980	1000	1371	1750

Figure 9 shows the damage prediction result and the damage identification errors with respect to the number of inductance tunings. Without data enrichment, the result indicates damage at false location (22nd element) with 4.3 % stiffness reduction. Since the damaged locations may not be known in advance in practical circumstances, and the structural health monitoring system may not be able to determine erroneous results, the incorrect predictions would mislead the following decisions for remedy. However, as the inductance tunings are applied, the damage prediction error gradually decreased and the final result correctly identified the damage at the 25th element with predicted stiffness loss (6.8%) close to the actual 8.3% value. These results verify that the

proposed approach of data enrichment significantly improves the damage identification accuracy under noise influence.

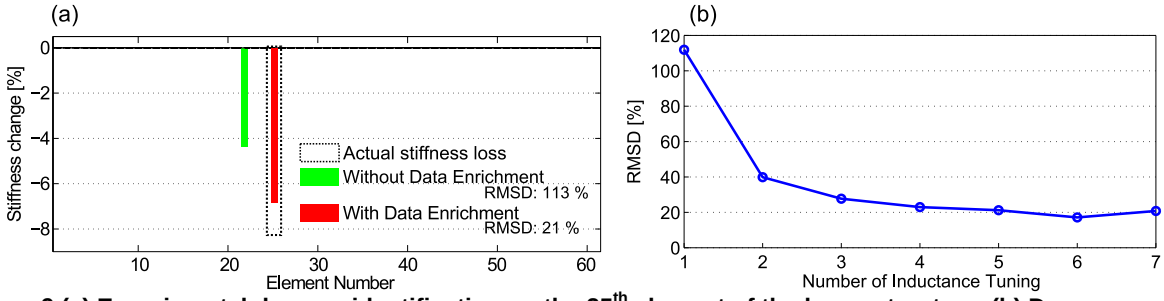

Figure 9 (a) Experimental damage identification on the 25th element of the beam structure. (b) Damage prediction error (RMSD) with respect to the number of inductance tunings.

Part III. Bayesian inference-based damage identification using piezoelectric admittance with adaptive circuitry

An important element in the research of piezoelectric impedance method is to evaluate the location and severity of damage using measurement data. While the spectral element method combined with the adaptive circuitry idea has exhibited excellent performance, for very complex structures the damage identification based on the inverse analysis of such formulation may still encounter difficulty, because of high computational cost and the usual under-determined nature of the problem. That is, for structures with complex geometry and very large size, the number of unknowns is generally very large. Taking uncertainties into account, several probabilistic approaches, e.g., perturbation method, Kriging predictor and random matrix theory, have been suggested to characterize the underlying property of engineering structures. The Bayesian inference approach has shown certain advantages. For instance, it can specify the model parameters with prior information in the form of probability density function (PDF), which may be viewed as imposing soft physical constraints to enable a unique and stable solution. Moreover, this approach allows the computation of any type of statistics of the model parameters to be identified.

In this part of research, we develop a new robust algorithm to conduct damage localization and identification based on piezoelectric impedance/admittance information. In particular, this algorithm is built upon the Bayesian inference framework, which employs forward analysis-based approach instead of inversion-based identification procedures. To facilitate such analysis, the tunable inductive circuitry is considered, in which the identification performance under different inductance tunings is evaluated and improved.

When applying Bayesian theorem for structural model updating, the hypothesis $\boldsymbol{\theta}$ is interpreted as the vector of parameters that need to be identified. $\mathbf{D}$ denotes the measured signature, which in this study is the electrical admittance of piezoelectric transducer. M denotes modeling assumptions, reflecting the existing experience and knowledge. We then have

$$p(\boldsymbol{\theta} \mid \mathbf{D}, M) = \frac{p(\mathbf{D} \mid \boldsymbol{\theta}, M)\, p(\boldsymbol{\theta} \mid M)}{\int p(\mathbf{D} \mid \boldsymbol{\theta}, M)\, p(\boldsymbol{\theta} \mid M) d\boldsymbol{\theta}} \tag{20}$$

The prior distribution $p(\boldsymbol{\theta}|M)$ expresses the initial knowledge of concerned parameters, e.g., stiffness, mass, and possible damage location. The choice of this distribution depends on how much information of the system is known. In this research, the parameters are only specified within certain range based on the prior information. Therefore, for the sake of simplicity, this term can be defined as a multivariate uniform distribution. The posterior distribution $p(\boldsymbol{\theta}|\mathbf{D},M)$ indicates the updated knowledge of the parameters $\boldsymbol{\theta}$ conditional on the prior knowledge and measured admittance information. The likelihood function $p(\mathbf{D}|\boldsymbol{\theta},M)$ is used to evaluate the agreement between the measurements and associated model output. Specifically, considering that uncertainties exist in real measurement, here we define the likelihood function as a multivariate normal distribution to conduct the screen of model output over $\boldsymbol{\theta}$ space.

$$p(\mathbf{D}|\boldsymbol{\theta}) = \frac{1}{\sqrt{(2\pi)^k |\Sigma|}} e^{-\frac{(\mathbf{D}-\mathbf{D}(\boldsymbol{\theta}))^T \Sigma^{-1} (\mathbf{D}-\mathbf{D}(\boldsymbol{\theta}))}{2}} \tag{21}$$

where $\mathbf{D}$ is a measured admittance vector having length k, and $\mathbf{D}(\boldsymbol{\theta})$ is the model output parameterized by $\boldsymbol{\theta}$. Σ is the covariance matrix of $\mathbf{D}$. Under this framework, the damage status of the structure monitored can be eventually identified.

Here we seek to localize and identify small-size damage in a plate structure. The host structure is an aluminum square plate ($0.5m \times 0.5m \times 0.005m$) attached with piezoelectric circuitry. The plate is clamped at its two ends, and modeled using plate finite elements. The piezoelectric transducer is a square one with length 0.0025m, which covers 25 (5×5) plate elements. An inductor is connected to the transducer, and its value is adjusted to 3.6662 H, in order to generate desired resonant effects. Assume damage occurs in a single element with 40% Young's modulus reduction, and is located near the center of the plate. As no prior knowledge of possible damage severity (reduction of element Young's modulus) and location is known, we choose bivariate uniform distribution as the prior distribution. The number of samples parameterized from such a distribution is equal to the product of the possible damage severity candidates and damage location candidates. In real situation, the damage severity candidates are continuously sampled within certain range, and damage can probably occur in each element of plate, which yields a large number of samples based on prior distribution. Based on the essence of Bayesian inference, repeated evaluation of the likelihood function corresponding to such samples using Monte Carlo simulation can be conducted, where evaluation of likelihood function depends on the harmonic

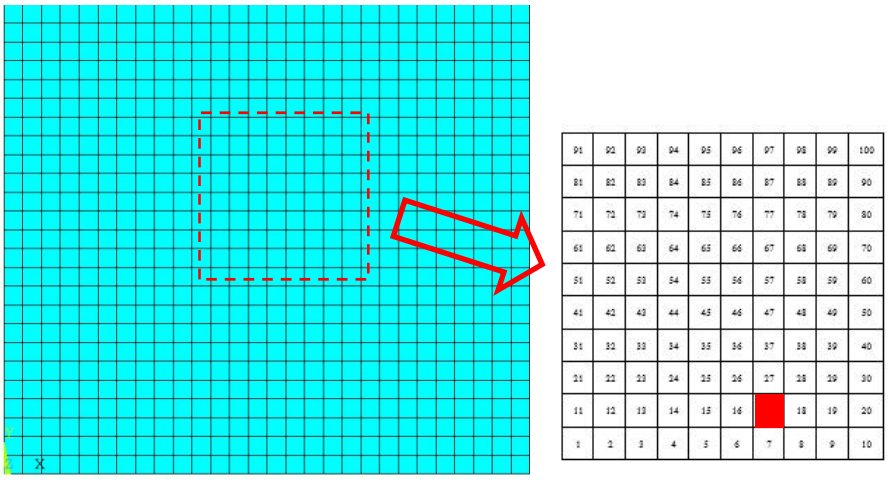

Figure 10 Damage scenario

response analysis with multiple excitation frequency components. For the purpose of illustration, here we consider a region of the plate where damage is assumed more likely to occur (including 100 elements marked by red circle in Figure 10). Moreover, the possible damage severity candidates are reduced to a vector [40% 60% 80%]. The interested frequencies range from 1060Hz to 1140Hz, generating uniformly distributed 50 frequency components. Although the damage severity does not continuously vary, we can use meta-modeling technique such as Gaussian process to interpolate and predict the posterior probabilities under unobserved damage severity candidates in the future study. Taking uncertainties into account, the 0.5% admittance measurement standard deviation is introduced to establish the likelihood function. Furthermore, in this case study, we demonstrate the results with respect to the different inductance values ($L_1 = 3.6662$ and $L_2 = 3.5662$), aiming at facilitating the identification process and further providing the adaptive inductance tuning guideline for practical experimental manipulation.

The posterior distributions obtained by using different inductance configurations can be seen in Figure 11. As such distribution inherently is high dimensional, we convert it into several low dimensional descriptions in order to highlight the comparison. It is worth mentioning that all the identified probability distributions in demonstrated figures are normalized. Based on this series of results, some observations can be summarized as follows.

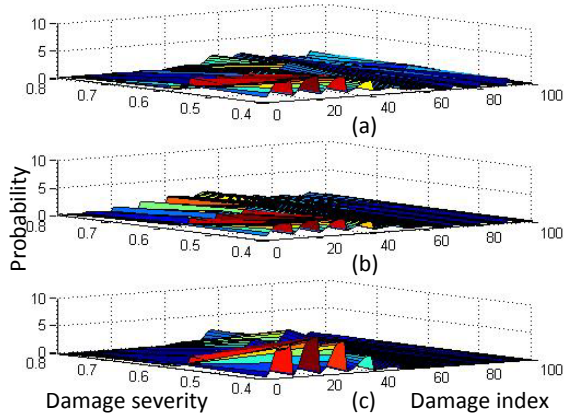

Figure 11 Posterior distribution versus damage severity and damaged element index: (a) with L_1, (b) with L_2, (c) combination of L_1 and L_2.

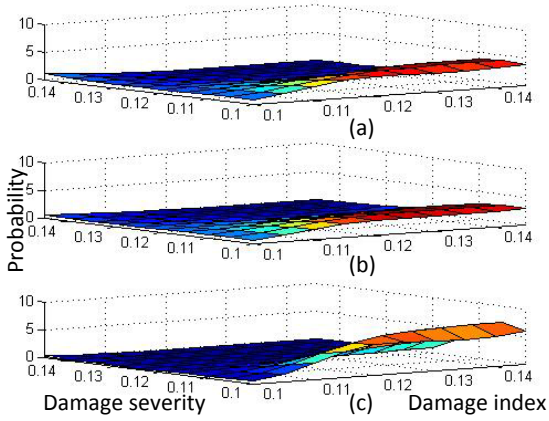

Figure 12 Posterior distribution of damage location under 40% severity: (a) with L_1, (b) with L_2, (c) combination of L_1 and L_2.

Under damage severity 40%, the identified distribution by using the information of both L_1 and L_2 becomes narrower, which indicates better identification performance as compared to that obtained by using admittance of individual L_1 or L_2 alone. However, under damage severity 60% or 80%, this identification enhancement is not that obvious. The reason is that the nominal damage severity for this case analysis is indeed pre-specified as 40%. In other words, other unreliable damage scenarios, e.g., damage severities 60% or 80%, cannot yield the increasing probability values even more admittance information is utilized. This is certainly in agreement with the underlying physical characteristics. The advantages of using the concept of tunable inductance circuitry are further analyzed by comparing the probabilities numerically. When employing the tunable inductance circuitry, several high fidelity scenarios have the increased likelihood (larger probability values), which clearly validates the feasibility of this underlying

idea. The identification performance under L_1 is better than that of L_2, which indicates that the inductance tuning technique plays an important role in conducting damage identification process.

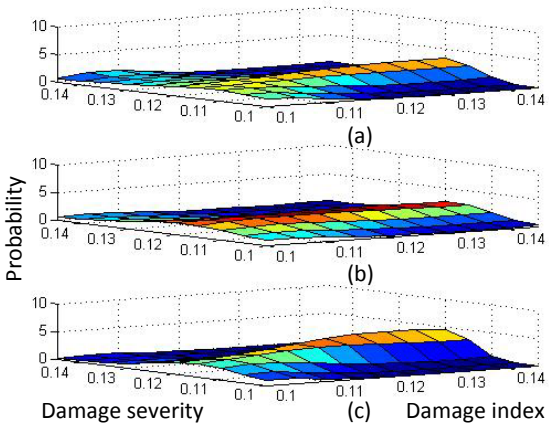

Figure 13 Posterior distribution of damage location under 60% severity: (a) with L_1, (b) with L_2, (c) combination of L_1 and L_2.

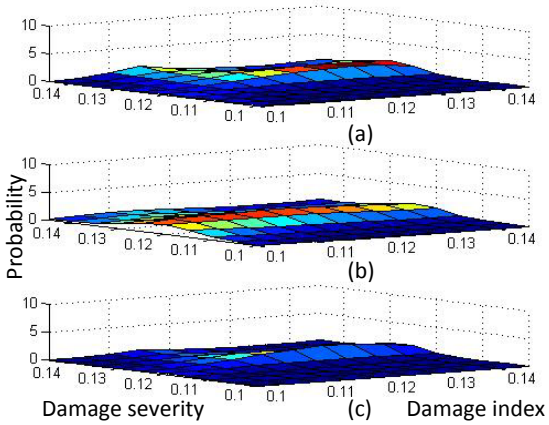

Figure 14 Posterior distribution of damage location under 80% severity: (a) with L_1, (b) with L_2, (c) combination of L_1 and L_2.

Personnel Supported

Other than the PIs, Drs. K. W. Wang and J. Tang, the project has involved three graduate students (Jinki Kim, Qi Shuai, and Kai Zhou).

Publications

Jinki Kim and K. W. Wang, "Impedance-Based Damage Identification Enhancement via Tunable Piezoelectric Circuitry," *SPIE Conferences on Smart Structures and Materials*, San Diego, CA, 2014.

Jinki Kim, R. L. Harne, and K. W. Wang, "Enhancing Damage Identification Robustness to Noise and Damping using Integrated Bistable and Adaptive Piezoelectric Circuitry," *ASME International Design Engineering Technical Conferences & Computers and Information in Engineering Conference*, DETC-2014-34993, Buffalo, NY, 2014.

Jinki Kim and K. W. Wang, "An Enhanced Impedance-Based Damage Identification Method using Adaptive Piezoelectric Circuitry," *Smart Materials and Structures*, Vol. 23, No. 9, p 095041.

Jinki Kim, R. L. Harne and K. W. Wang, "Enhancing Structural Damage Identification Robustness to Noise and Damping with Integrated Bistable and Adaptive Piezoelectric Circuitry," *ASME Journal of Vibration and Acoustics*, accepted for publication.

Q. Shuai, and J. Tang, "Lift-off Effect Compensation For Magnetic Impedance-based Damage Detection," *SPIE Conferences on Smart Structures and Materials*, San Diego, CA, 2014.

K. Zhou, Q. Shuai, and J. Tang, "Adaptive Damage Detection Using Tunable Piezoelectric Admittance sensor and Intelligent Inference," *ASME Conference on Smart Materials, Adaptive Structures and Intelligent Systems*, SMASIS-2014-7624, New Port, RI, 2014. (An improved version will be submitted to *Smart Materials and Structures*.)

Q. Shuai, and J. Tang, "Direct Compensation of Lift-Off Oscillation Effect in Magnetic Impedance-Based Damage Detection," *Journal of Intelligent Material Systems and Structures*, in revision.

Interactions/Transitions

This research is directly relevant to AFOSR's mission, since the results can be applied to various Air Force systems, such as aircraft fuselage, space structures, and gas turbine engines. The PIs have had various interactions and technical discussions with Dr. Mark Derriso at the Wright-Patterson Air Force Research Lab (AFRL) on issues regarding experimental set ups and DURIP ideas. Dr. Wang also has had communications with researchers at NASA Glenn. Dr. Tang has had extensive discussions with Pratt & Whitney engineers and GE Global Research Center

researchers to gather engineering insights on sensing mechanisms that have greatly enhanced the level of research.

Honors/Awards

Dr. K. W. Wang is the holder of the Stephen P. Timoshenko Collegiate Chair in Mechanical Engineering at the University of Michigan. He is a Fellow of the ASME, the Institute of Physics, and the American Association for the Advancement of Science. He has received numerous recognitions for his accomplishments; such as the SPIE Smart Structures and Materials Lifetime Achievement Award, the ASME Adaptive Structures and Materials Systems Prize, the ASME N. O. Myklestad Award, the ASME Adaptive Structures and Material Systems Best Paper Award, the ASME Rudolf Kalman Best Paper Award, the NASA Tech Brief Award, and the SAE Ralph Teetor Award. A recent paper by Jinki Kim, R. L. Harne, and K. W. Wang ("Enhancing Damage Identification Robustness to Noise and Damping using Integrated Bistable and Adaptive Piezoelectric Circuitry," *ASME International Design Engineering Technical Conferences & Computers and Information in Engineering Conference*, DETC-2014-34993, Buffalo, NY, 2014) has won the ***Second Place Best Student Paper Award*** at the *ASME Conference on Mechanical Vibration and Noise*.